

Spin Glass and Antiferromagnet Critical Behaviour in a Diluted fcc Antiferromagnet

Carsten Wengel^a, Christopher L. Henley^b, Annette Zippelius^a

^a*Inst. f. Theoretische Physik, Georg-August-Universität, 37073 Göttingen, Germany*

^b*Department of Physics, Cornell University, Ithaca, NY 14853*

Abstract

In this paper we report on a Monte Carlo study of a diluted Ising antiferromagnet on a fcc lattice. This is a typical model example of a highly frustrated antiferromagnet, and we ask, whether sufficient random dilution of spins does produce a spin glass phase. Our data strongly indicate the existence of a spin glass transition for spin-concentration $p < 0.75$: We find a divergent spin glass susceptibility and a divergent spin glass correlation length, whereas the antiferromagnetic correlation length saturates in this regime. Furthermore, we find a first order phase transition to an antiferromagnet for $1 \geq p > 0.85$, which becomes continuous in the range $0.85 > p > 0.75$. Finite size scaling is employed to obtain critical exponents. We compare our results with experimental systems as diluted frustrated antiferromagnets as $\text{Zn}_{1-p}\text{Mn}_p\text{Te}$.

arXiv:cond-mat/9509056v2 12 Sep 1995

I. INTRODUCTION

The family of diluted magnetic semiconductors (DMS) of the general form $A_{1-p}^{II}Mn_pB^{VI}$ encompasses a wide variety of alloys which have been under extensive investigation during the past 15 years. These alloys form a zincblende structure, where the B^{VI} element occupies one fcc lattice while A^{II} and Mn share the second fcc lattice. One fundamental aspect of research has focused on the magnetic order of these systems, since they offer practical examples of strongly frustrated, randomly diluted three dimensional fcc Heisenberg antiferromagnets (afm) with dominant nearest neighbour interaction^{1,2}.

In this paper we present results of a Monte Carlo study of a diluted frustrated Ising model on a fcc lattice given by the Hamiltonian

$$\mathcal{H} = -J \sum_{\langle i,j \rangle} \epsilon_i \epsilon_j s_i s_j, \quad \epsilon_i = \begin{cases} 1 & \text{with prob. } p \\ 0 & \text{with prob. } 1 - p. \end{cases} \quad (1)$$

Here, J is the coupling constant, which we will set $J = -1$ henceforward, and $p \in [0, 1]$ is the probability that a lattice site i is occupied with an Ising-spin s_i . We are interested in the static properties of this model for different dilution regimes. Besides the pure ($p = 1$) and the slightly diluted case ($p \sim 1$), that has already been studied by MC simulation³⁻⁵ and other methods^{6,7}, we concentrate our interest on the strong dilution regime, which has only been investigated in experimental Heisenberg-systems as mentioned above. Although in our work we perform a simulation of an Ising system we find that some typical DMS results can be reproduced with our simplified model.

Neutron diffraction experiments of thin $Zn_{1-p}Mn_pTe$ films for $p \in [1.0, 0.85]$ revealed a first order phase transition to an antiferromagnetically ordered state of ‘‘Type-III’’⁸. At approximately $p = 0.85$ a tricritical point is encountered, where the phase transition becomes continuous. The antiferromagnetic order in the regime $p \in [0.75, 0.85]$ is truly long range, however, below $p \approx 0.75$ a transition to a short range ordered phase seems to appear^{8,9}.

Below $p = 0.7$ most experimental results have led to the view, that one encounters a transition to a spin-glass-like phase at a fairly well defined temperature T_c . Characteristic spin

glass features are: (i) remanence effects in the frozen state^{10,11}, (ii) a pronounced cusp in the susceptibility around T_c ¹² with strong frequency dependence of the cusp temperature¹¹, (iii) absence of long range spin order as observed by magnetic neutron diffraction⁹, (iv) dynamic scaling near T_c of frequency-dependent response function^{13–16} and — most importantly — (v) a divergent nonlinear susceptibility around the cusp temperature¹⁷.

On the other hand, the antiferromagnetic correlation length ξ_{AFM} grows continuously with decreasing temperature until it saturates at the cusp temperature to an enormously large value as high as 70 Å at $p = 0.7$; it is only below $p = 0.4$ that short range afm order disappears. In the intermediate dilution range $p \in (0.4, 0.7)$ the spin glass interpretation has been questioned, and it was suggested briefly¹¹ (on the basis of an “activated” scaling analysis) that the equilibrium transition at T_c was to the antiferromagnetically ordered state of a random-field system.

This motivates a numerical study of a diluted antiferromagnet, in which we can observe the interplay of strong afm local order with spin glass order, and can measure the quantities now considered to be the signatures for spin-glass transitions. Because Heisenberg model simulations demand more computer time, and because of the more convoluted controversies regarding the existence of a sharp phase transition for continuous spins, we adopt here an Ising model; in addition, we have retained only the first-neighbour exchange interaction.

The paper is organized as follows: Section II is concerned with the main theoretical arguments that guide our expectations for the results of our simulations in the distinct dilution regimes. In particular, we discuss the possible universality class of the proposed spin glass phase. Section III describes technical aspects of our simulations, in particular the equilibration criterion. In section IV–VI of our report we shall present representative data for the distinct dilution regimes. In section IV we concentrate on the pure case and on weak dilution ($p \sim 1$), where we investigate how the order of the transition is being modified by disorder in form of stochastically removing spins from the lattice. Section V is concerned with the regime $p = 0.8$, where a continuous phase transition with afm ordering is found; critical exponents are determined by finite size scaling. Section VI investigates the

intermediate and strong dilution range ($p \in [0.3, 0.7]$), where the question of the magnetic ordering is our main concern. A summary of the results, a comparison to experimental systems and our final conclusions will be given in section VII.

II. THEORETICAL BACKGROUND

In this section, we collect the qualitative expectations for all the different concentration regimes expected in the phase diagram. As with the results in the subsequent sections, we begin by reviewing the pure case and proceed in the direction of greater dilution. The global phase diagram is qualitatively similar to those conjectured for *vector* spins in Ref. 18 and Ref. 19, except of course that distinctive collinear and noncollinear phases cannot exist in the Ising case.

A. Pure fcc Ising antiferromagnet

The pure Ising antiferromagnet on a fcc lattice has been extensively studied both analytically and with simulations. Each spin has 12 nearest neighbours which in the ground state can only satisfy 8 bonds, 4 of them being always violated. This effect of frustration, which follows from the triangles in the fcc lattice, leads to a large ground state degeneracy²⁰ of the order $\mathcal{O}(2^L)$, where L denotes the linear extent of the system. Thus the entropy per spin is zero as $L \rightarrow \infty$.

At small temperatures in this system, thermal fluctuations generate free energy terms which have the same effect as ferromagnetic second neighbor interactions: this favors the “Type-I” afm order, meaning that the system orders into one of the six periodic ground states with a $\langle 100 \rangle$ type ordering wavevector⁶. This is an example of what Villain called “ordering due to disorder”²¹.

The discrete choice between the three $\langle 100 \rangle$ type directions suggests a similarity in behavior to the 3-state Potts model, which has a weakly first order phase transition in three dimensions. Indeed, the $4 - \epsilon$ renormalization group predicts a first-order phase transition²².

Simulations^{4,5,23} and series expansions⁷ confirm that the phase transition is at finite temperature and is of first order.

The antiferromagnetic state may be handled quantitatively by constructing (in the spirit of Ref. 24) a three-component staggered-magnetization order parameter $\mathbf{m}^\dagger = (m_1^\dagger, m_2^\dagger, m_3^\dagger)$ with components

$$m_\mu^\dagger = \frac{1}{N} \sum_j \exp(-i \mathbf{r}_j \cdot \mathbf{k}_\mu) s_j \quad (2)$$

for $\mu = 1, 2, 3$; here the ordering wave vectors are $\mathbf{k}_1 = (\pi, 0, 0)$ and cyclic permutations (We have taken the lattice constant to be unity.).

B. Weak dilution: random-field effects

Dilution in frustrated systems (without any external field) couples to the order parameter as a random field does in a ferromagnet^{25,18}. Take the case of rather weak dilution, which justifies assuming (as a sort of variational state) one of the six $\langle 100 \rangle$ type ground states. Consider the effect of strengthening one *bond* lying within the xy plane: it will favor the four states with (100) and (010) ordering wavevectors and disfavor the two with (001) wavevectors, since the bond in question is violated in the (001) states. The effect is much like a random field, except that it does not destroy the global up/down symmetry. In our case of *site* dilution, the random-field-like effects of removing an isolated site cancel each other; however, removing a *pair of sites* has the same effect as would strengthening the bond between them^{26,25}.

Quite generally, when the random field is sufficiently strong, the first-order transition is converted to a continuous one²⁷. In the present context, since the effective random field grows with dilution, this argument predicts a tricritical point: the ordering transition is first-order for $p > p_{tri}$ but becomes continuous for $p < p_{tri}$ ²⁸.

For $p < p_{tri}$ the transition from the paramagnet is expected to be a novel universality class²⁷. It would seem plausible if its dynamic scaling behavior were of the “activated” type,

as in the random-field Ising model. No experiments have tested this, however (The materials in this concentration range, roughly $0.7 < p < 0.85$, can be grown only as thin epitaxial slabs, meaning that very little signal is available for susceptibility experiments.). A claim was made that “activated” scaling could fit the data¹¹ for lower values of p , which we would identify as the spin-glass phase, but this was quickly corrected^{13,15,16}.

When the “effective random fields” are sufficiently strong, the antiferromagnetic order disappears and is replaced by spin-glass order at a critical value p_* ²⁹. Note that this threshold to propagate afm order is far above the p_c , the geometrical percolation threshold for propagating connectivity of nearest-neighbor sites³⁰ (On the fcc lattice, $p_c = 0.195$ ³¹).

C. Spin glass phase

Any spin glass, by definition, requires random frustration. This can be realized by dilution of a uniformly frustrated antiferromagnet, as in the present case, just as well as by a random mix of ferromagnetic and antiferromagnetic interactions²¹. Indeed, the effective coupling between two spins may be ferromagnetic or antiferromagnetic depending on how intervening sites happen to be occupied. Of course, this spin glass state is expected to show residual short-range correlations as opposed to the cases of the $\pm J$ or Gaussian random bond distributions, where symmetry implies that $[\langle s_i s_j \rangle] = 0$ if $i \neq j$.

It is intriguing that this “spin glass” state, which occurs below p_* , from the viewpoint of the antiferromagnetic phase, is the same as the disordered domain state which is favored by the “effective random fields” mentioned above³². This state is different from the familiar random-field disordered state (and similar to the usual spin glass state) because the global up/down symmetry is preserved; consequently, for $p < p_*$ there is still a true phase transition in which this symmetry is broken³³.

D. Universality

In a concentration range (p'_c, p_*) , the ground state is presumed to be a spin glass. Spin glass investigations tend still to be preoccupied with the issue of the existence of a transition as a function of dimension, external field, and spin type. Indeed, it is still unsettled whether the $d = 3$ Ising spin glass really has a transition at finite temperature, or whether it is at the lower critical dimensionality^{34,35}. Rather little has been done to test the universality of the critical exponents, as almost all simulations have used simple cubic (sc) lattices with the discrete $\pm J$ distribution of random bonds. Monte Carlo and series studies for the fcc lattice with $\pm J$ bonds³⁶ gave values of the spin-glass exponents η , ν , and γ consistent with the sc $\pm J$ model; so did *diluted* $\pm J$ model on a simple cubic lattice³⁷ and (modulo large error bars) Gaussian-distributed random bonds on the simple cubic lattice³⁴. The above results are consistent with universality. However, it has also been proposed that η is more negative and the Binder cumulant is larger for Gaussian bond randomness than for $\pm J$ randomness³⁸; presumably the diluted fcc is more similar to the latter model, since its discrete randomness generically allows exact degeneracy of ground states.

E. Theory of p'_c (spin glass near percolation)

We now consider the approach $p \rightarrow p'_c$, where the spin glass long-range order finally disappears. In this regime, the order is just barely propagating along tortuous, effectively one-dimensional paths, and consequently we expect $T_c \rightarrow 0$ (exponentially) as $p \rightarrow p'_c$ ^{39,37}.

Note that $p'_c > p_c$. In frustrated models with discrete bond distributions, such as the present case, two portions of a connected cluster might be connected by (say) two chains of bonds, each canceling the other and allowing one portion to be flipped relative to the other portion at no cost in energy; for propagation of order, it is as if no chain existed, i. e., the effective concentration of bonds is lowered by the cancellations.

III. TECHNICALITIES

We use the single spin flip Monte Carlo Metropolis algorithm in our simulations. Spins are updated sequentially and randomly. Periodic boundary conditions are imposed, limiting the possible lattice sizes to even numbers. Spins are represented on a cubic lattice with next nearest neighbour interactions to obtain a fcc lattice. Therefore, every lattice of linear size L contains $N = L^3/2$ sites. We simulated lattice sizes $L = 4, 6, 8, 10$ with $M \approx 120$ realizations of the disorder and $L = 16$ with $M = 40$. We investigate the model in the concentration range $p \in [0.3, 1.0]$.

A standard criterion by Bhatt and Young⁴⁰ was applied to test the equilibration of the systems throughout the whole simulation, where we observe a continuous phase transition. The procedure is to obtain two estimates of the spin glass phase indicator, the spin glass susceptibility

$$\chi_{\text{SG}} = \frac{1}{N} \sum_{ij} [\langle s_i s_j \rangle^2] \quad (3)$$

Here and later, the brackets $\langle \dots \rangle$ denote thermal averaging and $[\dots]$ configurational averaging. We obtain χ_{SG} by calculating the second moment of the spin glass order parameter defined in the two alternative ways, (i) as the overlap

$$q_{12}(t, t_0) = \frac{1}{N} \sum_i s_i^{(1)}(t_0 + t) s_i^{(2)}(t_0 + t) \quad (4)$$

and (ii) as the autocorrelation (self-overlap)

$$q_{\nu}(t, t_0) = \frac{1}{N} \sum_i s_i(t_0 + t) s_i(t_0 + t + t'). \quad (5)$$

Here, $s_i^{(1)}$ and $s_i^{(2)}$ denote two sets of spins (replicas) with the same set of occupied sites and uncorrelated initialization and t_0 is the time initially used for equilibration.

With these definitions, we can compute two estimates of χ_{SG} as follows, i. e.,

$$\chi_{\text{SG}}^{(a)} = \left[\left\langle \frac{1}{N} \left(\sum_i s_i^{(1)}(t_0 + t) s_i^{(2)}(t_0 + t) \right)^2 \right\rangle_{\tau} \right], \quad (6)$$

respectively the four-spin correlation function,

$$\chi_{\text{SG}}^{(b)} = \left[\left\langle \frac{1}{N} \left(\sum_i s_i(t_0 + t) s_i(2t_0 + t) \right)^2 \right\rangle_{\tau} \right], \quad (7)$$

where $\langle \dots \rangle_{\tau} = \frac{1}{\tau} \sum_1^{\tau} (\dots)$, and $\tau = t_0$.

The equilibration time t_0 was raised on a logarithmic scale and we only accepted a run, if both estimates of χ_{SG} agreed after this time within certain limits, typically of the order of 5% of their joint mean value. The longest runs performed were up to $2 * 10^6$ Monte Carlo steps per spin (MCS). Most of the simulations were performed on HP workstations at the Institut für Theoretische Physik, Göttingen and on the Intel–Paragon parallel computer at the Höchstleistungsrechenzentrum Jülich. The program was parallelised by using *PVM 3.2* software⁴¹ in order to simulate many systems simultaneously.

IV. FIRST ORDER ANTIFERROMAGNETIC TRANSITION (WEAK DILUTION)

In this section we investigate the pure afm and the slightly diluted regime, i. e., $p \in [0.85, 1.0]$. We wish to determine the order of the phase transition and how the order of the transition is changed by introducing disorder into the system in form of slight stochastic dilution. The magnetic order in this regime is clearly antiferromagnet, consistent with earlier simulations, and shall be closer examined in section V.

The pure antiferromagnet on a fcc lattice is known to undergo a temperature driven first order phase transition^{3,4,23,5,7}, as mentioned in the previous section. Early Monte Carlo simulations by Grest and Gabl³ as well as Giebultowicz¹⁹ reported a change from a first order to a continuous phase transition upon dilution. Grest and Gabl located the tricritical point at a critical concentration $p_{\text{tri}} = 0.93$ using Ising–spins, whereas Giebultowicz found a slightly lower $p_{\text{tri}} = 0.85$ with a Heisenberg–spin simulation. However, in both of those simulations, no averaging over the disorder was performed, so that we re–investigated this regime.

An important quantity for a first order phase transition is the internal energy density

$$[\langle e \rangle] = \left[\left\langle \frac{1}{2N} \sum_{\langle i,j \rangle} \epsilon_i \epsilon_j s_i s_j \right\rangle \right]. \quad (8)$$

At the critical temperature, this quantity indicates a first order phase transition by a discontinuity (latent heat), which can be seen in Fig. 1, where $[\langle e \rangle]$ is plotted versus temperature T ; with increasing lattice size a pronounced discontinuity at the transition temperature can be observed, revealing clearly a first order transition.

In Fig. 2 we present our data of the internal energy density for $p = 0.9$. For this concentration the transition appears to be continuous. Apparently, a tricritical point is hard to locate with these Monte Carlo data, since it is not clear, whether in the limit of smaller temperature steps and larger systems the transition will turn out to be continuous or not. In order to determine the tricritical concentration more efficiently we used a method first introduced by Lee & Kosterlitz⁴², which is based on a histogram algorithm by Ferrenberg & Swendsen⁴³.

A. Histogram algorithm and finite-size scaling analysis method

This method⁴³ uses one long Monte Carlo run to estimate the free energy at several temperatures close to T_c . During the runs a histogram of the internal energy density e is accumulated. This histogram serves as an estimate of the equilibrium energy distribution (after correct normalization)

$$P_\beta(e) = \frac{1}{Z_\beta} \exp(S(e) - \beta e). \quad (9)$$

Here, Z_β is the partition function at the inverse temperature $\beta = 1/k_B T$ and $S(e)$ is the entropy. Notice, that $P_\beta(e)$ (9) is proportional to $\exp(-\beta F(e))$, where F denotes the free energy. The distribution $P_\beta(e)$ can now be used to generate the distribution (and consequently $F(e)$) at a different inverse temperature β' in the vicinity of β .

We are interested in the situation in which $F(e)$ has two minima e_1 and e_2 (i.e. (9) has maxima at these energies). The temperature at which $F(e_1, L) = F(e_2, L)$ is taken

to be the effective critical temperature for the given size L . Then we evaluate the “gap” $\Delta F = F(e_m) - F(e_{1,2})$ between the free energy values at those two energies and at the maximum e_m in between them. From a scaling analysis of ΔF , one can identify whether a phase transition is first order⁴².

A state with $e \in [e_1, e_2]$ consists of a domain of ordered and a domain of disordered phase coexisting, separated by a $(d - 1)$ -dimensional interface surrounding the droplet of minority phase. Therefore, one can expand the free energy

$$F(e, L) = L^d f_0(e) + L^{d-1} f_1(e) + \mathcal{O}(L^{d-2}), \quad (10)$$

where the bulk free energy density f_0 is minimal and constant for $e \in [e_1, e_2]$ and the surface term f_1 is maximal at $e_1 < e_m < e_2$. Expansion (10) is valid for any first order phase transition, as long as the correlation length $\xi < L$. At the critical temperature ξ remains finite, so that for sufficiently large L the appearance of a free energy gap ΔF indicates a first order transition; for small $L < \xi$ the free energy is dominated by the bulk term. As the system approaches a tricritical point, ξ grows and the double minima structure can only be seen for large L . At a tricritical point and beyond it, the phase transition is continuous and hence there is no double minimum structure for any L .

B. Results

To obtain good statistics, we took histogram data every 10^{th} MCS for 6×10^6 MCS, averaging over 16 realizations of the disorder.

Fig. 3 shows two histograms of the internal energy density for $p = 1$ after normalization for two different temperatures (full and dashed line). The dots were produced by transforming the $T = 1.77$ data set (dashed line) to the lower temperature $T = 1.74$. The distribution depends sensitively on the chosen temperature; the Monte Carlo data at $T = 1.74$ and the transformed data from $T = 1.77$ show good agreement, indicating, that the equilibrium distribution has been well estimated. The simulation temperature in Fig. 3 was chosen very

close to the critical temperature. Therefore, as noted above, the distribution clearly has two maxima at e_1 and e_2 , which are equivalently minima of $F(e)$.

If we define the effective critical temperature $T_c(L)$ by the equality of the two maxima $P_\beta(e_1)$ and $P_\beta(e_2)$ and extrapolate $T_c(L \rightarrow \infty)$, we obtain $T_c(p = 1.0) = 1.716(5)$. This is slightly lower than the values from Ref. 5 ($T_c = 1.736(1)$) and Ref. 7 ($T_c = 1.746(5)$). This discrepancy may be due to using different definitions of “finite-size T_c ” in the respective references.

While for $p = 1$ the energy gap appears already at $L = 10$, for stronger dilution it can only be seen at larger system sizes, indicating the growing correlation length as one approaches the tricritical point. If a gap appeared at one system size, it continued to be present and in fact grew for larger sizes. The scaling behaviour according to eq. (10), i. e., $\Delta F(L) \propto L^2$, is fulfilled within the error margins. In the diluted case we found considerable fluctuations of the energy gap size depending on the realization. At $p \sim 0.9$ for our largest systems ($L = 22$) certain realizations were found, that showed none of the typical two peak structure, while others still showed a small gap.

In order to determine the tricritical dilution p_{tri} , we evaluated the percentage of realizations with gap ($= Y$) with decreasing concentration of spins. For our largest systems ($L = 22$), at $p = 0.91$ $Y = 90\%$ of the realizations still showed a double peak, at $p = 0.9$ only 40%, at $p = 0.89$ 10% and for $p = 0.88$ no double peaks were found at all, i. e., all systems showed Gaussian peaks at T_c . From extrapolating $(T_c(L), p_{\text{tri}}(L))$ determined by the condition $Y = 0.5$ for different system sizes (see dots in Fig. 10), we estimated $p_{\text{tri}} = 0.85 \pm 0.03$ in accordance with Ref. 19. To determine the tricritical concentration more exactly would require a precise scaling analysis based on more extensive data, which was beyond the scope of this work.

V. CONTINUOUS ANTIFERROMAGNETIC TRANSITION ($P = 0.8$)

In this section we concentrate on simulations performed for $p = 0.8$. Our aim is to check, whether at T_c the system orders into an antiferromagnetic state and, since we are below the tricritical concentration we measure critical exponents via finite size scaling close to the continuous phase transition, that we encounter.

A. Quantities analysed

For the antiferromagnetic phase, the staggered magnetization “vector” \mathbf{m}^\dagger (see eq. 2) is the appropriate order parameter. Thus, we calculate the second moment

$$m^2 = [\langle \mathbf{m}^\dagger \cdot \mathbf{m}^\dagger \rangle]. \quad (11)$$

For $T > T_c$ this is proportional to the staggered susceptibility $\chi^\dagger = Nm^2$, which we analysed by using the finite size scaling form

$$\chi^\dagger(L, T) = L^{2-\eta} \tilde{\chi}^\dagger(L^{1/\nu}(T - T_c)) \quad (12)$$

to extract the critical exponents η and ν and the critical temperature T_c .

Since we are mainly interested in the magnetic order of the different dilution regimes, we also calculated correlation functions. To save computer time, we Fourier transform the lattices to k -space and calculate the Fourier transformed correlation function, i. e.,

$$G(\mathbf{k}) = [\langle |s_{\mathbf{k}}|^2 \rangle] = \frac{1}{N} \sum_{ij} \exp(-i \mathbf{r}_{ij} \cdot \mathbf{k}) [\langle s_i s_j \rangle]. \quad (13)$$

We applied the Fast Fourier algorithm to the (most relevant) $L = 16$ systems only and calculated the correlation function along the three $\langle 100 \rangle$ directions. For an antiferromagnet, the three $k = \pi$ modes of G should yield the static staggered susceptibility, which we used as a consistency check. The correlation length ξ can be extracted from the knowledge of the scaling form of G , i. e.,

$$G(k) = \frac{1}{k^{2-\eta}} \tilde{G}(k\xi). \quad (14)$$

The scaling factor \tilde{G} has the following asymptotics: For $k > 0$ and $T \rightarrow T_c^+$, $\tilde{G}(k\xi) \rightarrow 1$ and for $T > T_c$ and $k \rightarrow 0$ (in the afm case $k = \pi - k'$ with the limit $k' \rightarrow \pi$)

$$\begin{aligned} G(k \rightarrow 0) &\sim \frac{1}{k^{2-\eta}} (k\xi)^{2-\eta} = \xi^{2-\eta} \\ &\sim (T - T_c)^{-\nu(2-\eta)} = (T - T_c)^{-\gamma} \\ &\sim \chi. \end{aligned} \tag{15}$$

In eq. (15) we have used the scaling form of the correlation length $\xi \sim (T - T_c)^{-\nu}$ and the scaling law $\gamma = \nu(2 - \eta)$. With this knowledge of the asymptotic form of G we chose the Ansatz

$$G(k) = \frac{1}{k^{2-\eta}} \tilde{G}(k\xi) = \frac{A}{k^{2-\eta} + \xi^{\eta-2}}, \tag{16}$$

that we used to fit our data of the correlation function in order to obtain an estimate for ξ and η . The constant A has been introduced as the amplitude of the correlation function.

Finally we shall analyse the heat capacity

$$C = \frac{N}{T^2} [\langle e^2 \rangle - \langle e \rangle^2]. \tag{17}$$

This quantity indicates a continuous phase transition to an ordered state by a weak divergence at the critical temperature. We use the finite size scaling form

$$C(L, T) = L^{\alpha/\nu} \tilde{C}(L^{1/\nu}(T - T_c)) \tag{18}$$

to extract critical exponents α and ν as well as T_c .

B. Results

Our data of the staggered magnetization show an increasing m^2 (eq. 11) as T approaches the critical temperature, becoming more pronounced for larger lattice sizes. This contribution to the afm order parameter can as well be seen in the divergent behaviour of the staggered susceptibility (Fig. 4). The scaling analysis⁴⁴ of the staggered susceptibility yields

$T_c(p = 0.8) = 1.07 (0.05)$, $\nu = 0.51 (0.1)$ and $\eta = 0.05 (0.1)$. The data scale well over a wide temperature range with the exception of the $L = 4$ data and the errors in the exponents are within acceptable limits.

The antiferromagnetic correlation length ξ_{AFM} is found to grow continuously with decreasing temperature and reaches half the lattice size at $T \approx 1.2$, before the critical temperature $T_c = 1.07$. Since finite size effects become appreciable at distances close to half the lattice size, we only included data above $T = 1.2$ for a fit of the scaling form $\xi \sim (T - T_c)^{-\nu}$. We extracted $\nu = 0.55$ by regression, which is in good agreement with our previous result. From fitting the correlation function to eq. (16), we were also able to extract a second estimate of η ; here, we found $\eta = -0.04$ with a slow drift to $\eta \rightarrow -0.02$ for $T \rightarrow 1.2$.

We do not perform a complete finite size scaling analysis of the correlation function in this work, because it would require a substantial amount of additional data for larger lattice sizes. Therefore, our estimates for the exponents obtained from $G(k)$ are less reliable than those obtained from finite size scaling. Nevertheless, this analysis serves as an additional consistency check and the critical exponents lie well within the error margins of those exponents obtained via finite size scaling of the susceptibility.

The heat capacity shows a weak divergence at the critical temperature at $p = 0.8$. Fig. 5 displays the best result of the scaling procedure according to eq. (18) with $T_c = 1.08 (0.05)$, $\nu = 0.57 (0.1)$ and $\alpha = 0.38 (0.15)$. These exponent values satisfy the hyperscaling relation

$$d\nu = 2 - \alpha \tag{19}$$

with $\nu = 0.54$ in 3 dimensions.

In summary, the dilution regime $p = 0.8$ exhibits a continuous phase transition to an antiferromagnetically ordered state. We obtained critical exponents using finite size scaling; however, since $p = 0.8$ is very close to the tricritical point, it is quite possible that these are only effective exponents from the crossover between the mean field exponents of the tricritical point ($\eta = 0$, $\nu = 1/2$ and $\alpha = 1/2$) to whatever universality class is appropriate for the continuous ordering transition. With the data at hand this question has to remain

open.

VI. SPIN GLASS ORDER

Upon further dilution we encounter a dramatic change in the magnetic order of the system at the phase transition. We investigate the question, whether below $p = 0.8$ the system really orders into a spin glass or if antiferromagnetic ordering can still be found. First, we introduce the spin glass order parameter and the spin glass susceptibility. Then we discuss our data at $p = 0.7$, and proceed with results from simulations of stronger diluted systems.

A. Theory and quantities measured

Besides the quantities that have been introduced in the previous section, we also measured the standard indicator of a spin glass transition, the spin glass susceptibility χ_{SG} (see eq. (3)). For an infinite system a spin glass transition is signalled by a divergence of χ_{SG} as $(T - T_c)^{-\gamma}$, with $\gamma = (2 - \eta)\nu$. For our scaling analysis, χ_{SG} is computed as the second moment of the overlap, defined by eq. (4) and eq. (6). We analysed our estimate of the spin glass susceptibility by using its finite size scaling form

$$\chi_{\text{SG}}(L, T) = L^{2-\eta} \tilde{\chi}_{\text{SG}}(L^{1/\nu}(T - T_c)). \quad (20)$$

Another important quantity, that is well-known in the analysis of spin glass simulation data⁴⁰, is the Binder cumulant⁴⁵ of the spin glass order parameter

$$g = \frac{1}{2} \left(3 - \frac{[\langle q^4 \rangle]}{[\langle q^2 \rangle]^2} \right). \quad (21)$$

It has the pleasant finite size scaling form

$$g(L, T) = \tilde{g}(L^{1/\nu}(T - T_c)) \quad (22)$$

with no power of L multiplying \tilde{g} , which makes it very valuable for precise scaling analysis. The Binder cumulant (21) is defined so that $0 \leq g \leq 1$, and above T_c , $g(L, T) \rightarrow 0$ for

$L \rightarrow \infty$. In particular, the intersection of all $g(L, T)$ curves at some point provides an accurate estimate of T_c .

To investigate a change of magnetic order further, we analysed the correlation function again, this time also the spin glass correlation function

$$G_{\text{SG}}(\mathbf{k}) = [\langle |q_{\mathbf{k}}|^2 \rangle] = \frac{1}{N} \sum_{i,j} \exp(-i \mathbf{r}_{ij} \cdot \mathbf{k}) [\langle q_i q_j \rangle]. \quad (23)$$

Here, we defined $q_i = s_i^{(1)}(t + t_0) s_i^{(2)}(t + t_0)$. The same fitting procedure of our data was employed as in the previous section in order to compute the respective correlation length, ν and η .

B. Results for intermediate dilution ($p = 0.7$)

The (antiferromagnetic) staggered susceptibility as shown in Fig. 6, is drastically reduced in comparison to Fig. 4, and shows only a small tendency to increase as T decreases. Furthermore, scaling according to eq. (12) could not be achieved for reasonable parameters.

On the other hand our data reveal a divergence of χ_{SG} at $p = 0.7$ of the same order of magnitude as χ^\dagger for $p = 0.8$ in Fig. 4. This divergence becomes particularly strong for larger lattice sizes in the vicinity of $T = 0.85$. If χ_{SG} is the critical quantity for this system then it should also scale according to eq. 20.

A finite size scaling analysis of the spin glass susceptibility is given in Fig. 7. All data for χ_{SG} with the exception of $L = 4$ scale well with $T_c(p = 0.7) = 0.85$ (0.05), $\nu = 1.0$ (0.2) and $\eta = 0.1$ (0.2). The fact that the spin glass susceptibility satisfies the above scaling form (20) strongly suggests that the magnetic order of this model has changed between $p = 0.8$ and $p = 0.7$ from antiferromagnet to spin glass.

In Fig. 8 we present our data of g at $p = 0.7$. The data show the typical behaviour as it has been observed in short range spin glasses, i. e., the data merge at approximately $T = 0.85$, indicating the phase transition. There is even a slight tendency of fanning out of the data below this intersection point, which is a strong evidence for the occurrence of a phase

transition. Such a fanning out is usually observed in uniform systems. In our system this may be due to the proximity to the tricritical point or to residual short range antiferromagnetic order (see below). The best fit was achieved with $T_c(p = 0.7) = 0.83 (0.05)$ and $\nu = 1.05(0.2)$, which agrees well with our estimates from the scaled spin glass susceptibility. The stronger scattering of this quantity, especially of the $[\langle q^4 \rangle]$ data, may be due to insufficient disorder averaging (40 systems for $L = 16$) and could probably be decreased with additional computational power.

In Fig. 9 the temperature dependence of ξ_{SG} and ξ_{AFM} are presented. While the spin glass correlation length is very small for large T but increases drastically as $T \rightarrow T_c \approx 0.83$, the antiferromagnetic correlation length starts at a higher level but increases slower than ξ_{SG} ; it ceases to increase at about $T = 0.9$ and saturates for lower temperatures.

All these results of our simulations at $p = 0.7$ are consistent with the interpretation that in this dilution regime we witness indeed a spin glass transition, but also encounter antiferromagnetic order of long but *finite* range being embedded into long range spin glass order. Apparently, a change of magnetic order has taken place within the interval $p_* \in (0.7, 0.8)$, where p_* denotes the critical dilution, where this change happens.

C. Results for strong dilution

Additional simulations were performed for concentrations $p = \{0.6, 0.5, 0.4, 0.3\}$. With stronger dilution we find that the spin glass phase already encountered for $p = 0.7$ persists. Both, spin glass susceptibility and Binder cumulant of the order parameter scale well in this regime with slight dilution dependent critical exponents. Also, in this regime the data of the Binder cumulant stay together below T_c for all sizes, as has been observed in other short range Ising spin glass simulations. Unfortunately, it is increasingly difficult in this regime to equilibrate the systems. As the concentration is lowered, the critical temperature decreases rapidly (as expected from our argument earlier, that $T_c(p'_c) = 0$ with $p'_c > p_c = 0.195$), but the characteristic microscopic energy barriers remain of order unity. Metastability becomes

an increasingly important problem and is prohibitive in large systems. In our simulations, for $p < 0.6$ we were unable to equilibrate the $L = 16$ systems sufficiently close to T_c within reasonable computer time.

From analysing the correlation function in the strong dilution regime we find two results: First, the spin glass correlation length shows a similar divergence close to the critical temperature for $p = \{0.6, 0.5, 0.4\}$ as we have seen in the previous subsection, confirming again the development of long range spin glass order. Second, we still find short range antiferromagnetic order, which decreases with lower concentration: for $p = 0.6$ ξ_{AFM} rises slowly when T is lowered and at T_c we have $\xi_{\text{AFM}} \approx 4$; for $p = 0.4$ the correlation length remains constant at $\xi_{\text{AFM}} \approx 2$ for all temperatures which we can simulate ($T \in [0.56, 1.0]$, $T_c(p = 0.4) \approx 0.47$).

Furthermore, both critical exponents ν and η apparently decrease with increasing dilution (see the fitted values in table I). The generic theoretical expectation is that the exponents should be universal all along the spin glass transition line, but the issue of universality is not completely settled in diluted systems⁴⁶. In our case, we note that the drift in the exponents is pronounced for $0.5 < p < 0.7$ but minimal for $0.5 \geq p \geq 0.3$. Thus we suggest that this dependence is an artifact of the antiferromagnetic correlation length, which is large and p -dependent for $0.5 < p < 0.7$, but is quite small for $0.3 < p < 0.5$. However, we have insufficient information to check this proposition, and shall come back to this issue in the conclusion.

We conclude, that for the whole range $p \in [0.3, 0.7]$ our simulations testify the existence of a spin glass phase transition for the short range antiferromagnetic Ising model on a fcc lattice. Simultaneously, the model also exhibits residual antiferromagnetic order, that is relatively long ranged at $p = 0.7$ and saturates close to the critical temperature; it decreases with further dilution, showing no temperature dependence for $p = 0.4$.

VII. CONCLUSION

In this paper we have presented a Monte Carlo simulation of the diluted short range antiferromagnetic Ising model on a fcc lattice. The main purpose was to investigate the thermodynamic equilibrium properties of this model.

In the undiluted case ($p = 1$) we have found a first order phase transition to an antiferromagnetically ordered state, consistent with earlier simulations. Upon slight dilution, the antiferromagnetic order persists, the first order transition becoming weaker and changing to a continuous transition at the tricritical concentration $p_{\text{tri}} \approx 0.85$. At $p = 0.8$ we still find antiferromagnetic order from analysis of the correlation function and scaling of the staggered susceptibility. Together with scaling of the heat capacity, we find mutually consistent critical exponents. The question of universality remains unclear; in view of the proximity to $p_{\text{tri}} \approx 0.85$ it seems likely that we observe tricritical exponents at this point.

Below $p = 0.8$ the divergence of the spin glass correlation length as well as scaling of the spin glass susceptibility and the Binder cumulant of the order parameter signal spin glass order. This means, that there must be a multicritical point at some concentration $p_* \in (0.7, 0.8)$, where the change of magnetic order takes place. Simultaneously, the quasi temperature independent staggered magnetization and the saturation of the antiferromagnetic correlation length suggest the breakdown of antiferromagnetic long range order. The fact, that the antiferromagnetic correlation length saturates while spin glass correlations still grow contradicts the view of a dynamically inhibited transition to an antiferromagnet. Rather, our data suggest that the coexistence of antiferromagnetic short range order together with long range established spin glass order seems to be a special phenomena of this diluted model.

Let us now turn to the question of universality in the spin glass phase. In this phase (see Sec. VI) our scaling fits yielded critical exponents slightly dependent on dilution (compare table I); we speculated, that this could be an artifact of the changing antiferromagnetic correlation length. Even in unfrustrated models, there is still controversy over the univer-

sality of exponents under dilution⁴⁶. Although our simulations are less extensive than the MC-simulations of the short range Ising spin glass by Bhatt and Young and by Ogielski, it is interesting to compare our exponents with their values for the $\pm J$ -model in $d = 3$. For this model, they find^{40,48} $\nu \approx 1.2$ and $\eta \approx -0.25$. These values are just at or slightly out of the error margins of the present simulations, so that it is not entirely clear, whether the two models lie in the same universality class. Note also, that our value of γ is smaller than for the “classic” spin glass simulations, roughly $\gamma \approx 1.8$ for $p \in [0.3, 0.7]$. Additional simulations of larger systems would be desirable to confirm our result.

It should be noted that even the best current simulations on hypercubic lattices have not put to rest the basic question whether the lower critical dimension for Ising spin glasses is below 3, or equal to 3^{40,48,34,36,35,38}. At the more modest scale of our simulation, it cannot be decisively answered whether the diluted fcc Ising antiferromagnet has a genuine spin glass transition, and if so whether it has precisely the same exponents as the standard example of $\pm J$ spin glasses on hypercubic lattices using array processors. However, our data is consistent with both of these propositions.

Although in this work we have performed an Ising model simulation we find striking similarities with experimental observations in DMS, which have Heisenberg like magnetic moments⁴⁷. Not only are the respective phase diagrams (compare Fig. 10 and Ref. 8) qualitatively similar and the various critical concentrations are numerically close, but also the concentration dependence of ξ_{AFM} in the spin glass phase agrees well with experiment. To be more specific, a comparison of our simulations with intensive experimental studies by Giebultowicz et al.⁸ on $\text{Zn}_{1-p}\text{Mn}_p\text{Te}$ shows the following agreements: (i) the afm transition is first order for $p \in [0.85, 1.0]$, (ii) the transition is continuous (to an afm long-range state) for $p \in [0.75, 0.85]$, (iii) the afm order is of large but finite range for $p < p_* \approx 0.75$ in the spin glass phase and (iv) the afm correlation length decreases with increasing dilution $p < p_*$. These results together with the measured divergence of the nonlinear susceptibility in $\text{Cd}_{1-p}\text{Mn}_p\text{Te}$ (see Ref. 17) below $p_* \approx 0.75$ do support the view of a spin glass phase in experimental Heisenberg systems.

ACKNOWLEDGMENTS

C. W. and A. Z. would like to thank Reiner Kree for helpful discussions and J. Holm for his assistance. C. W. and A. Z. gratefully acknowledge support by SFB 345. C. L. H. is supported by NSF grant DMR-9214943.

TABLES

TABLE I. Critical quantities for different concentration p from scaling of the respective susceptibility, Binder cumulant and analysis of the respective correlation function. Not listed are the scaling results of the heat capacity for $p = 0.8$. They are: $T_c = 1.07 (0.05)$, $\alpha = 0.38 (0.1)$ and $\nu = 0.57 (0.1)$. With susceptibility and correlation function we denote the valid quantity for the respective dilution regime.

Critical Temperatures and Exponents				
Order	Concentration	Susceptibility	Binder cumulant	Correlation function
AFM	0.8	$T_c=1.07 (0.05)$		
		$\nu=0.51 (0.10)$		$\nu=0.55$
		$\eta=0.05 (0.15)$		$\eta = -0.04 (0.05)$
SG	0.7	$T_c=0.83 (0.05)$	$T_c=0.83 (0.05)$	
		$\nu=1.00 (0.20)$	$\nu=1.05 (0.20)$	$\nu=0.96$
		$\eta=0.10 (0.20)$		$\eta=0.15 (0.20)$
SG	0.6	$T_c=0.75 (0.05)$	$T_c=0.76 (0.05)$	
		$\nu=0.80 (0.20)$	$\nu=0.90 (0.20)$	$\nu=0.98$
		$\eta=0.00 (0.20)$		$\eta=0.07 (0.15)$
SG	0.5	$T_c=0.55 (0.05)$	$T_c=0.53 (0.05)$	
		$\nu =0.73 (0.20)$	$\nu =0.73 (0.20)$	
		$\eta = -0.30 (0.25)$		
SG	0.4	$T_c=0.47 (0.10)$	$T_c=0.44 (0.10)$	
		$\nu=0.80 (0.20)$	$\nu=0.80 (0.20)$	
		$\eta = -0.35 (0.20)$		
SG	0.3	$T_c =0.27 (0.10)$	$T_c =0.27 (0.10)$	
		$\nu =0.70 (0.20)$	$\nu =0.70 (0.25)$	
		$\eta = -0.40 (0.20)$		

REFERENCES

- ¹ T. M. Giebultowicz, J. J. Rhyne, W. Y. Ching, D. L. Huber, and J. K. Furdyna, *J. Appl. Phys.* **63**, 3279 (1988).
- ² J. K. Furdyna and N. Samarth, *J. Appl. Phys.* **61**, 3526 (1987).
- ³ G. S. Grest and E. G. Gabl, *Phys. Rev. Lett.* **43**, 1182 (1979).
- ⁴ M. K. Phani, J. L. Lebowitz, and M. H. Kalos, *Phys. Rev. B* **21**, 4027 (1980).
- ⁵ T. L. Polgreen, *Phys. Rev. B* **29**, 1468 (1984).
- ⁶ M. D. Mackenzie and A. P. Young, *J. Phys. C* **14**, 3927 (1981). See also: J. Slawny, *J. Stat. Phys.* **20**, 711, (1979).
- ⁷ D. F. Styer, *Phys. Rev. B* **32**, 393 (1985).
- ⁸ T. M. Giebultowicz, P. Kłosowsky, N. Samarth, H. Luo, J. K. Furdyna, and J. J. Rhyne, *Phys. Rev. B* **48**, 12817 (1993)
- ⁹ T. M. Giebultowicz, P. Kłosowsky, N. Samarth, H. Luo, J. J. Rhyne, and J. K. Furdyna, *Phys. Rev. B* **42**, 2582 (1990).
- ¹⁰ S. P. McAlister, J. K. Furdyna, and W. Girit, *Phys. Rev. B* **29**, 1310 (1984).
- ¹¹ S. Geschwind, A. T. Ogielski, G. Devlin, J. Hegarty, and P. Bridenbaugh, *J. Appl. Phys.* **63**, 3291 (1988).
- ¹² R. R. Galazka, S. Nagata, and P. H. Keesom, *Phys. Rev. B* **22**, 3344 (1980).
- ¹³ Y. Zhou, C. Rigeaux, A. Mycielski, M. Merant, and N. Bontemps, *Phys. Rev. B* **40**, 8111 (1989).
- ¹⁴ A. Mauger, J. Villain, Y. Zhou, C. Rigeaux, N. Bontemps, and J. Ferré, *Phys. Rev. B* **41**, 4587 (1990).
- ¹⁵ S. Geschwind, D. A. Huse, and G. E. Devlin, *Phys. Rev. B* **41**, 4854 (1990).

- ¹⁶ B. LeClercq, C. Rigaux, A. Mycielski, and M. Menant, Phys. Rev. B **47**, 6169 (1993).
- ¹⁷ A. Mauger, J. Ferré, and P. Beauvillain, Phys. Rev. B **40**, 862 (1989).
- ¹⁸ C. L. Henley, Phys. Rev. Lett. **62**, 2056 (1989).
- ¹⁹ T. M. Giebultowicz, J. Magn. Mag. Mat. **54–57**, 1287 (1986).
- ²⁰ A. Danielian, Phys. Rev. Lett. **6**, 670 (1964).
- ²¹ J. Villain, Z. f. Phys. B **33**, 31 (1979).
- ²² A renormalization-group approach could be formulated with a Landau–Ginzburg effective free energy as a function of the order-parameter field \mathbf{m}^\dagger . The fact that, in a particular ordered configuration, only one of the ordering wavevectors can be present, translates to a “cubic” anisotropy in order–parameter space favoring the three coordinate axes. This implies a first–order phase transition (see D. J. Wallace, J. Phys. C **6**, 1390 (1973)).
- ²³ K. Binder, J. L. Lebowitz, M. K. Phani, and M. H. Kalos, Acta Met. **29**, 1655 (1981).
- ²⁴ P. Bak, S. Krinsky, and D. Mukamel, Phys. Rev. Lett. **36**, 52 (1976). Also: D. Mukamel and S. Krinsky; Phys. Rev. B **13**, 5065 (1976), and S. A. Brazovskii, I. E. Dzyaloshinskii, and B. G. Kukharenko, Sov. Phys. JETP **43**, 1176 (1976) [Zh. Eksp. Teor. Fiz. **70**, 2257 (1976)].
- ²⁵ J. F. Fernandez, Europhys. Lett. **5**, 129 (1988).
- ²⁶ J. F. Fernandez, H. A. Farach, C. P. Poole, and M. Puma, Phys. Rev. B **27**, 4274 (1983).
- ²⁷ A. N. Berker, J. Appl. Phys. **70**, 5941 (1991).
- ²⁸ The general effect of introducing a random field is similar to a reduction in dimensionality. Now, models (such as the 3-state Potts model) which in $d = 3$ have weak first–order transitions as an effect of the many–component order parameter, tend to become second–order in $d = 2$. This would also lead us to predict a multicritical point; indeed, such a

point is observed in the Potts model (see S. Chen, A. M. Ferrenberg, and D. P. Landau, Phys. Rev. Lett. **69**, 1213 (1992), and compare also W. G. Wilson, Phys. Lett. A **137**, 398 (1989).)

²⁹ In principle, one could imagine a intermediate phase which had coexisting antiferromagnetic and spin glass order, which would thus have distinct critical concentrations p_* . That phase would be analogous to a state of two infinite interpenetrating percolation clusters, which is geometrically possible in $d = 3$. Within the rather coarse p grid of our simulations, however, only one p_* value is observed along the line $T = T_c(p)$.

³⁰ Y. Shnidman and D. Mukamel, Phys. Rev. B **30**, 384 (1984).

³¹ J. W. Essam, in *Phase Transitions and Critical Phenomena, Vol. II*, edited by C. Domb and M. Green (Academic, New York, 1971).

³² It is intriguing to speculate on the universality class of the transition as a function of p along the line $p_*(T)$. The afm order parameter would be expected to behave as in a random-field 3-state-Potts model (since the effective random fields distinguish among three ordering wavevectors) yet the spin glass order parameter would behave as at the spin-glass freezing temperature. Our simulations cannot address this question (which is best studied at $T = 0$).

³³ This situation is similar to the problem of propagating order in e.g. the 3-state Potts antiferromagnet on a triangular lattice, where a single chain of bonds is insufficient to force the relationship between two clusters (see J. Adler, R. G. Palmer and H. Meyer, Phys. Rev. Lett. **58**, 882 (1987), and H. Fried and M. Schick, Phys. Rev. B **41**, 4389 (1990). However, that problem is unfrustrated, in that the restriction of a pure system ground state to the sites of the diluted system is always *one* of the valid ground states; this is not true for a frustrated system such as the fcc antiferromagnet (compare Ref. 30) owing to its frustration and this complicates the propagation of order.

- ³⁴ R. N. Bhatt and A. P. Young, Phys. Rev. B **37**, 5606 (1988).
- ³⁵ E. Marinetti, G. Parisi and F. Ritort, J. Phys. A **27**, 2687 (1994).
- ³⁶ R. E. Hetzel, R. N. Bhatt, and R. R. P. Singh, Europhys. Lett. **22**, 383 (1993).
- ³⁷ S. Shapira, L. Klein, J. Adler, A. Aharony, and A. B. Harris, Phys. Rev. B **49**, 8830 (1994).
- ³⁸ L. Bernardi and I. Campbell, Phys. Rev. B **49**, 728 (1994).
- ³⁹ A. J. Bray and S. C. Feng, Phys. Rev. B **36**, 8456 (1987).
- ⁴⁰ R. N. Bhatt and A. P. Young, Phys. Rev. Lett. **54**, 924 (1985).
- ⁴¹ G. A. Geist et al., *PVM 3 Users Guide and Reference Manual*, Oak Ridge National Laboratory, Tennessee 37381, USA (1993).
- ⁴² J. Lee and J. M. Kosterlitz, Phys. Rev. Lett. **64**, 137 (1990).
- ⁴³ A. M. Ferrenberg and R. H. Swendsen, Phys. Rev. Lett. **61**, 2635 (1988).
- ⁴⁴ The listed errorbars of the critical exponents and the critical temperature are generous estimates from fitting the respective scaling form to our simulation data.
- ⁴⁵ K. Binder, Z. f. Phys. B **43**, 119 (1979).
- ⁴⁶ On the basis of simulations, it is argued by R. Kühn and A. Huber, Phys. Rev. Lett. **73**, 2268 (1994) and by J.-K. Kim and A. Patrascioiu, Phys. Rev. Lett. **72**, 2785 (1994), that the critical exponents of *unfrustrated* diluted Ising models show a non-universal dilution dependence.
- ⁴⁷ It is commonly believed that $d = 3$ is *below* the lower critical dimension for Heisenberg spin glasses, but anisotropic spin interactions — which are certainly present in DMS — are believed to drive the transition to the Ising class, even though the ordered state may be held together mainly by the isotropic interactions.

⁴⁸ A. T. Ogielski, Phys. Rev. B **32**, 7384 (1985).

FIGURES

FIG. 1. Internal energy density e versus temperature for $p = 1$.

FIG. 2. Internal energy density versus temperature for $p = 0.9$.

FIG. 3. The lines show two energy density distributions $P(e)$ versus energy density e for MC-simulations at two different temperatures, $p = 1.0$ and $L = 16$. The left peak corresponds to an antiferromagnetically ordered phase (low energy), the right peak to a paramagnetic phase, divided by an energy gap (latent heat). The points are calculated according to the Ferrenberg-Swendsen method from the high temperature distribution and agree well with the full line from low temperature MC-simulation.

FIG. 4. Staggered susceptibility χ^\dagger versus temperature, $p = 0.8$.

FIG. 5. Scaled heat capacity $CL^{-\alpha/\nu}$ versus $L^{1/\nu}(T - T_c)$, $p = 0.8$. Best scaling was achieved with $T_c = 1.08$ (0.05), $\nu = 0.57$ (0.1) and $\alpha = 0.38$ (0.1).

FIG. 6. χ^\dagger versus temperature, $p = 0.7$.

FIG. 7. $\chi_{SG}L^{2-\eta}$ versus $L^{1/\nu}(T - T_c)$, $p = 0.7$. Best scaling was achieved with $T_c = 0.83$ (0.05), $\nu = 1.0$ (0.2) and $\eta = 0.1$ (0.2).

FIG. 8. Binder cumulant of the spin glass order parameter versus temperature, $p = 0.7$.

FIG. 9. Spin glass correlation length ξ_{SG} (*) and antiferromagnetic correlation length ξ_{AFM} (●) versus temperature, $p = 0.7$.

FIG. 10. Phase diagram of the short range fcc Ising antiferromagnet with dilution. We plot T_c versus spin concentration p . We observed a 1^{st} order phase transition to an afm-state for $1.0 \geq p \geq p_{tri} \approx 0.85$ (long dashed line), becoming continuous for $p_{tri} \geq p \geq p_* \approx 0.75$ (dotted line). The dots above the transition line denote points $(T_c(L), p_{tri}(L))$ with the condition $Y = 50\%$ (see Sec. IV). Upon further dilution ($p \leq p_*$) we encountered a spin glass transition (full line, being extended down to the percolation threshold $p_c = 0.195$). The lines serves only to guide the eye. The gothic arch marks a region, where the order of the system is unknown (afm, spin glass or coexistence of both).

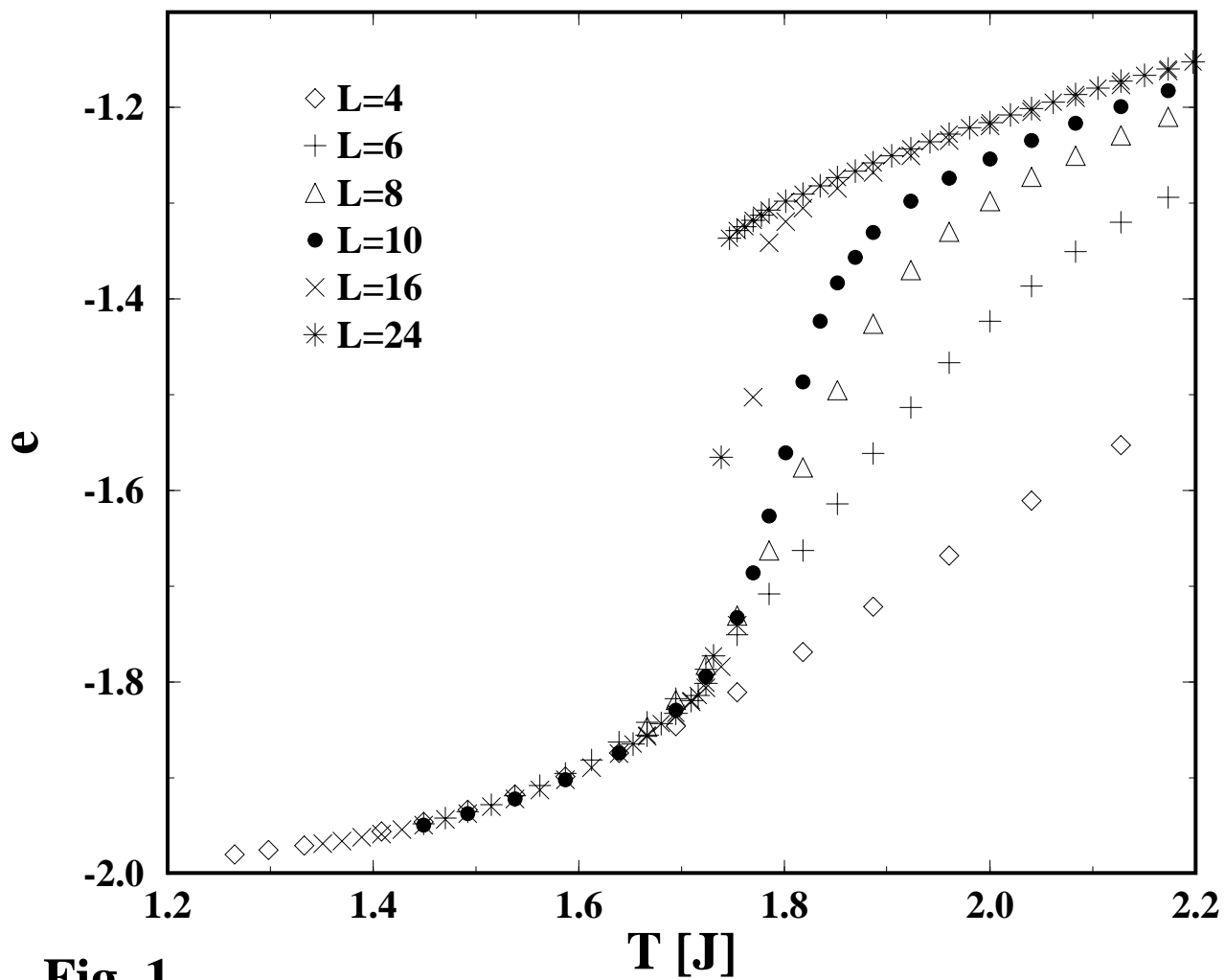


Fig. 1

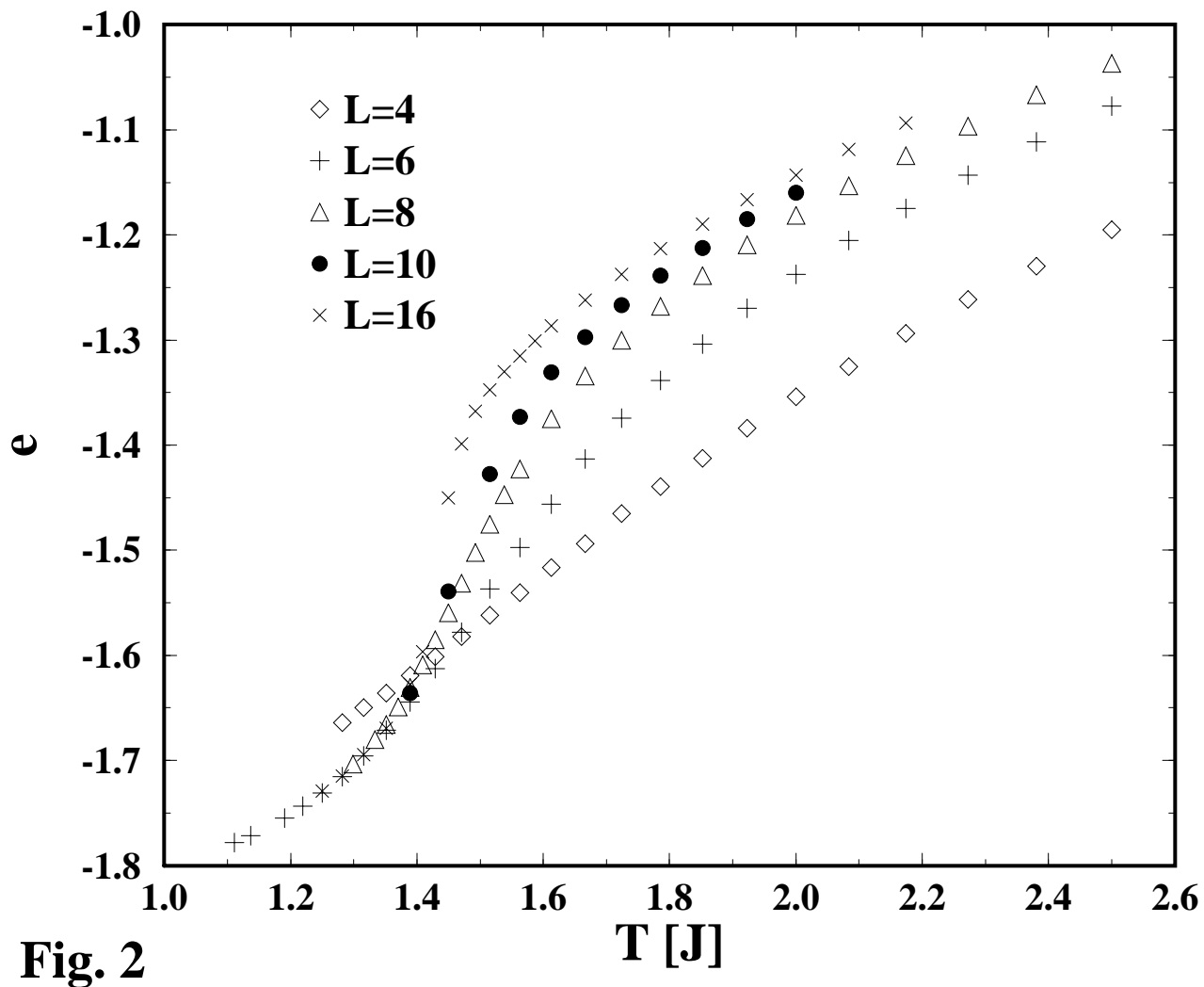


Fig. 2

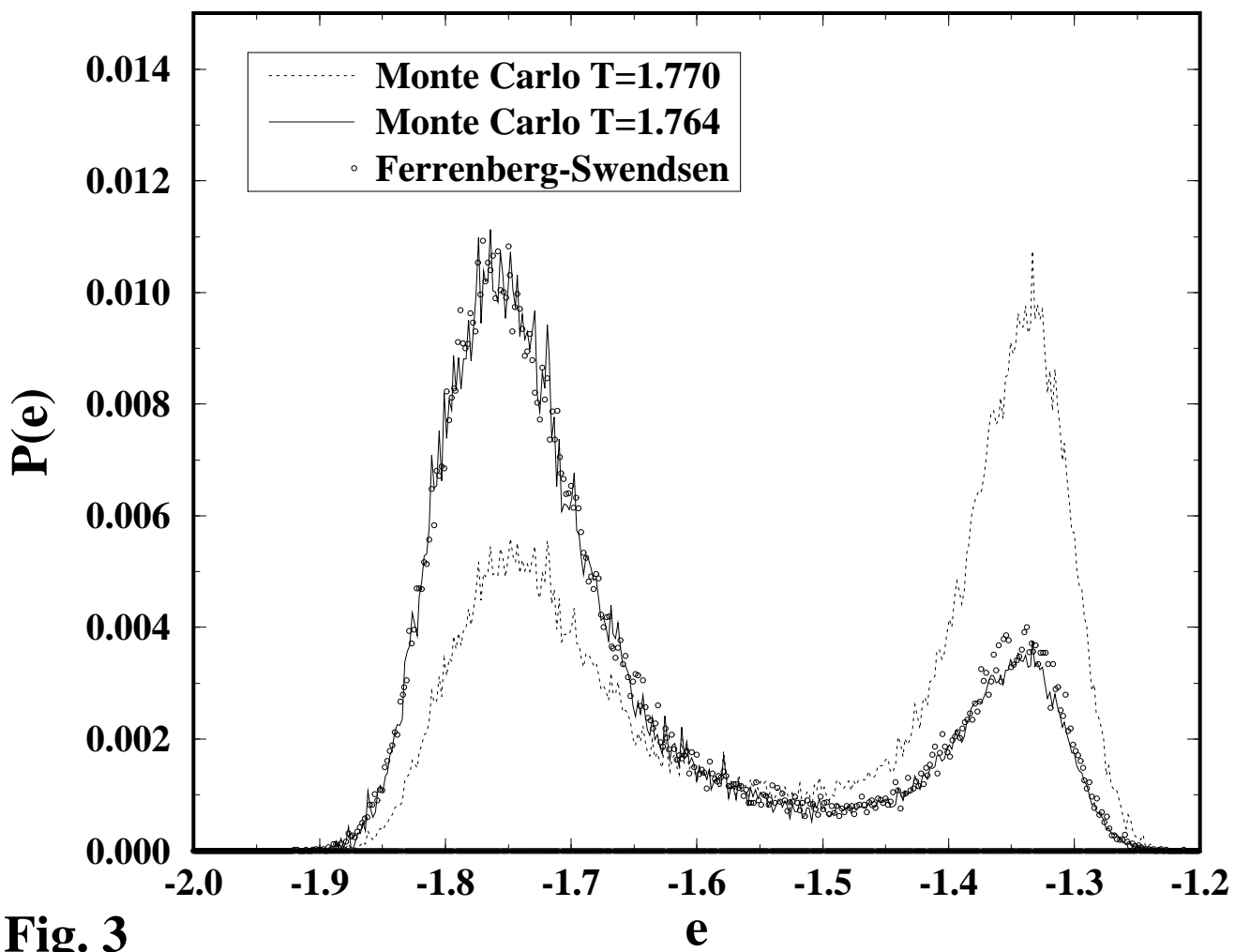


Fig. 3

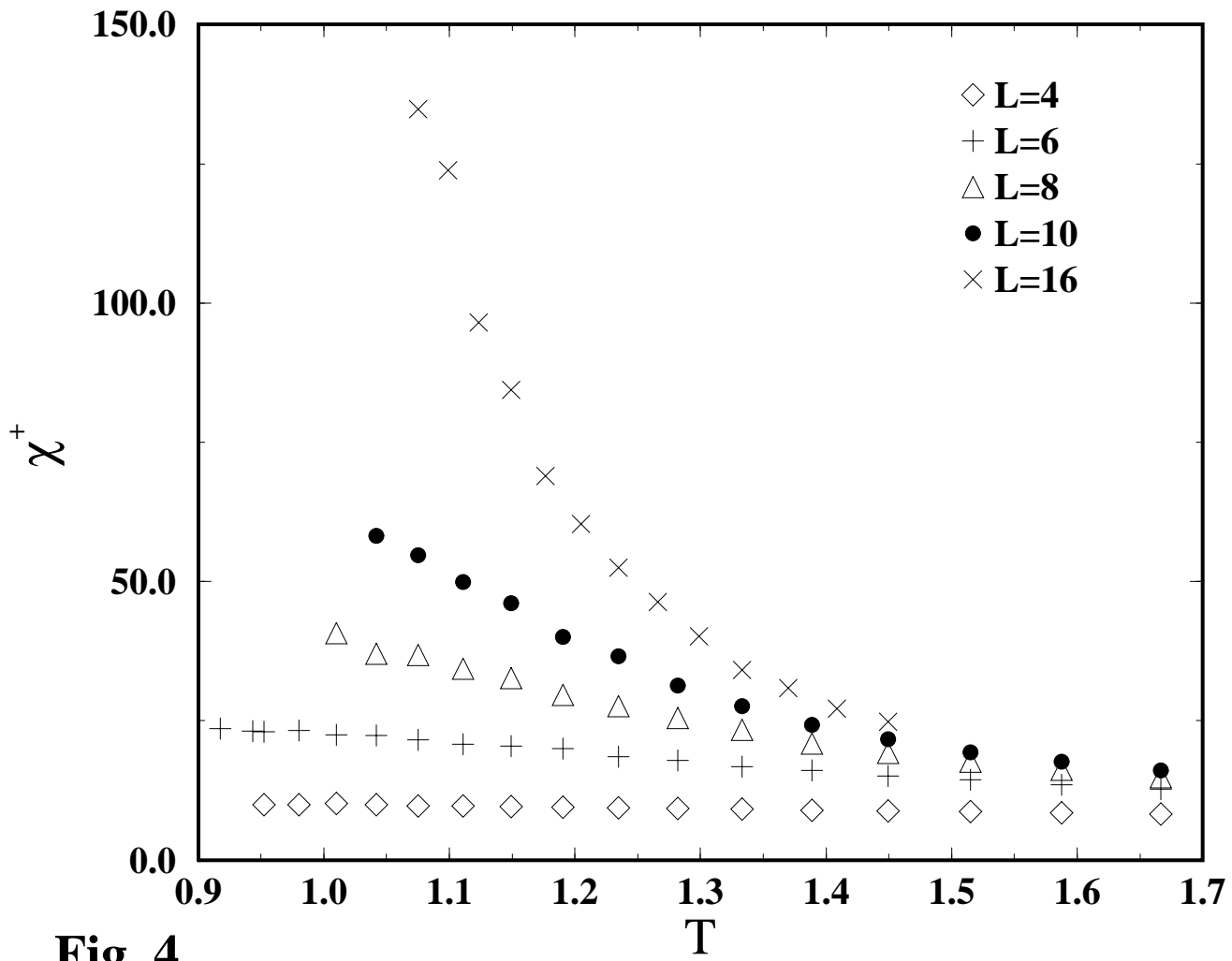


Fig. 4

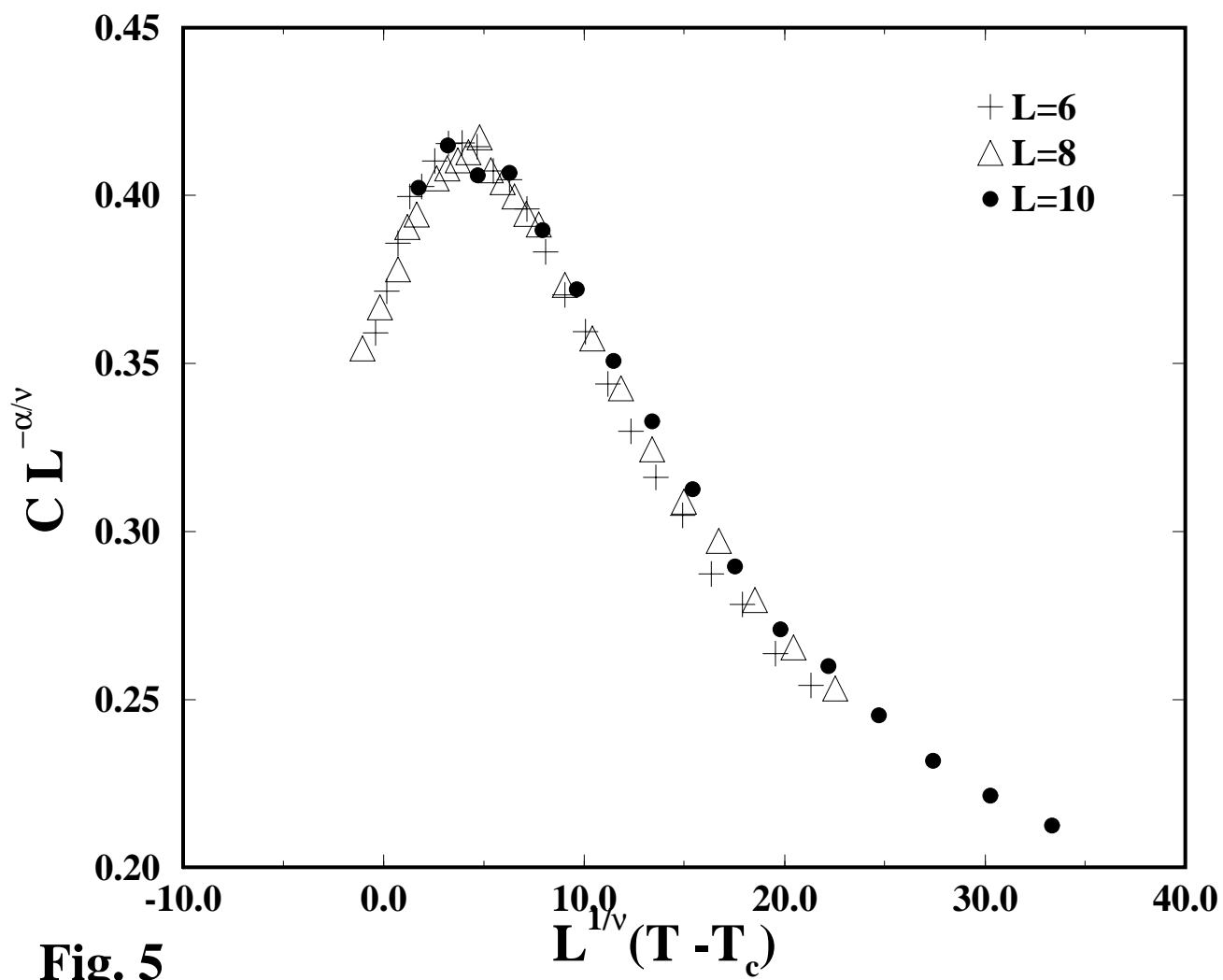


Fig. 5

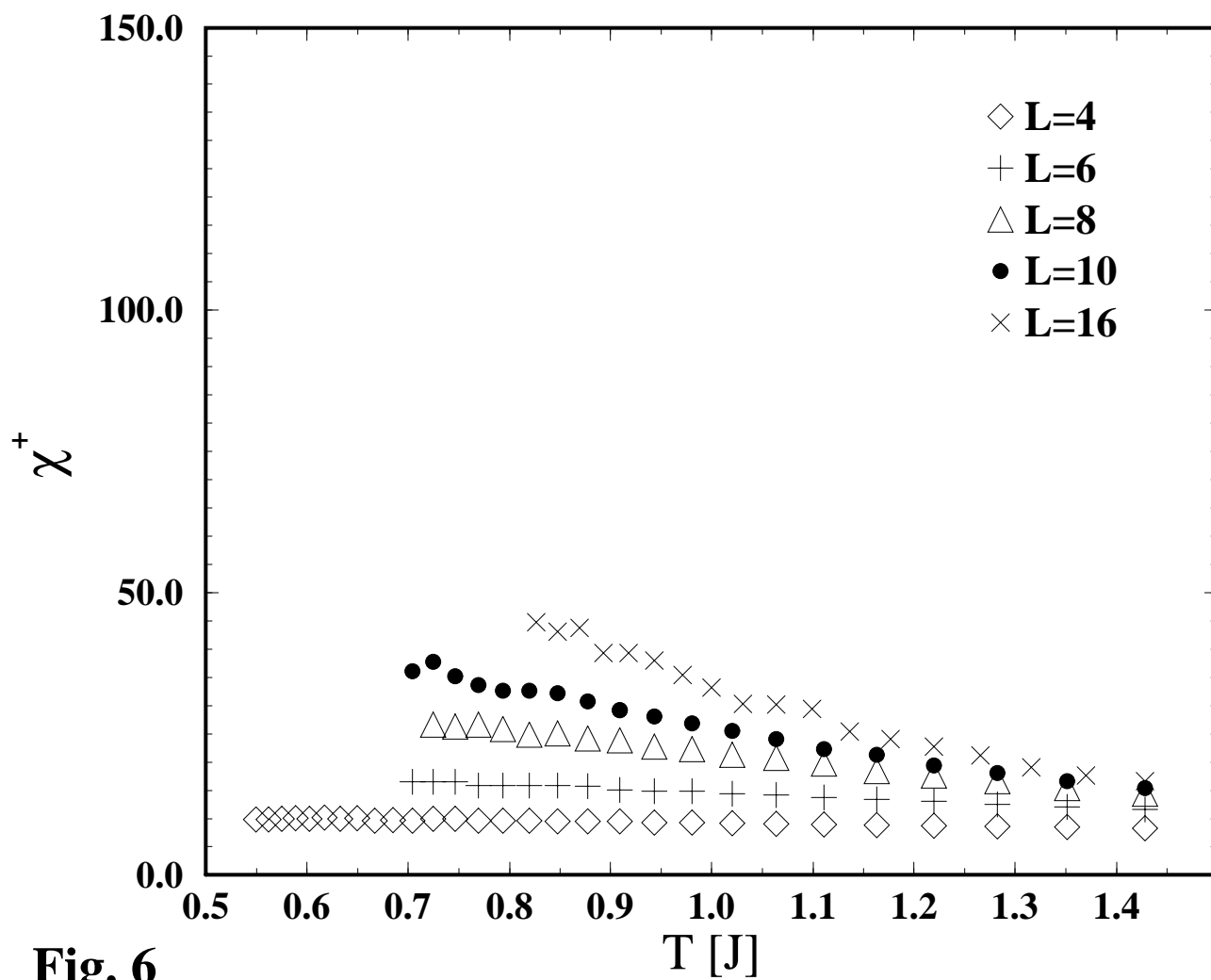


Fig. 6

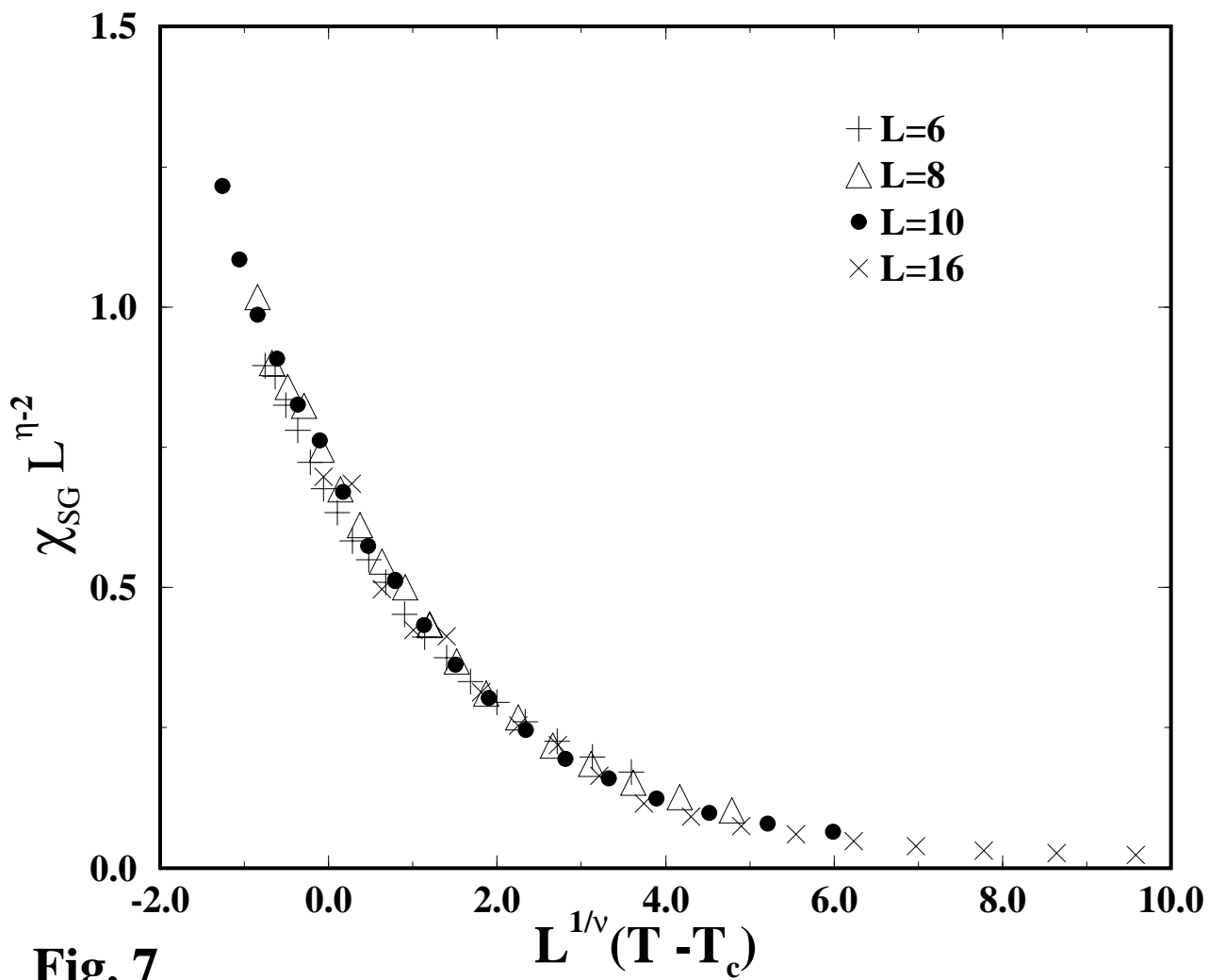


Fig. 7

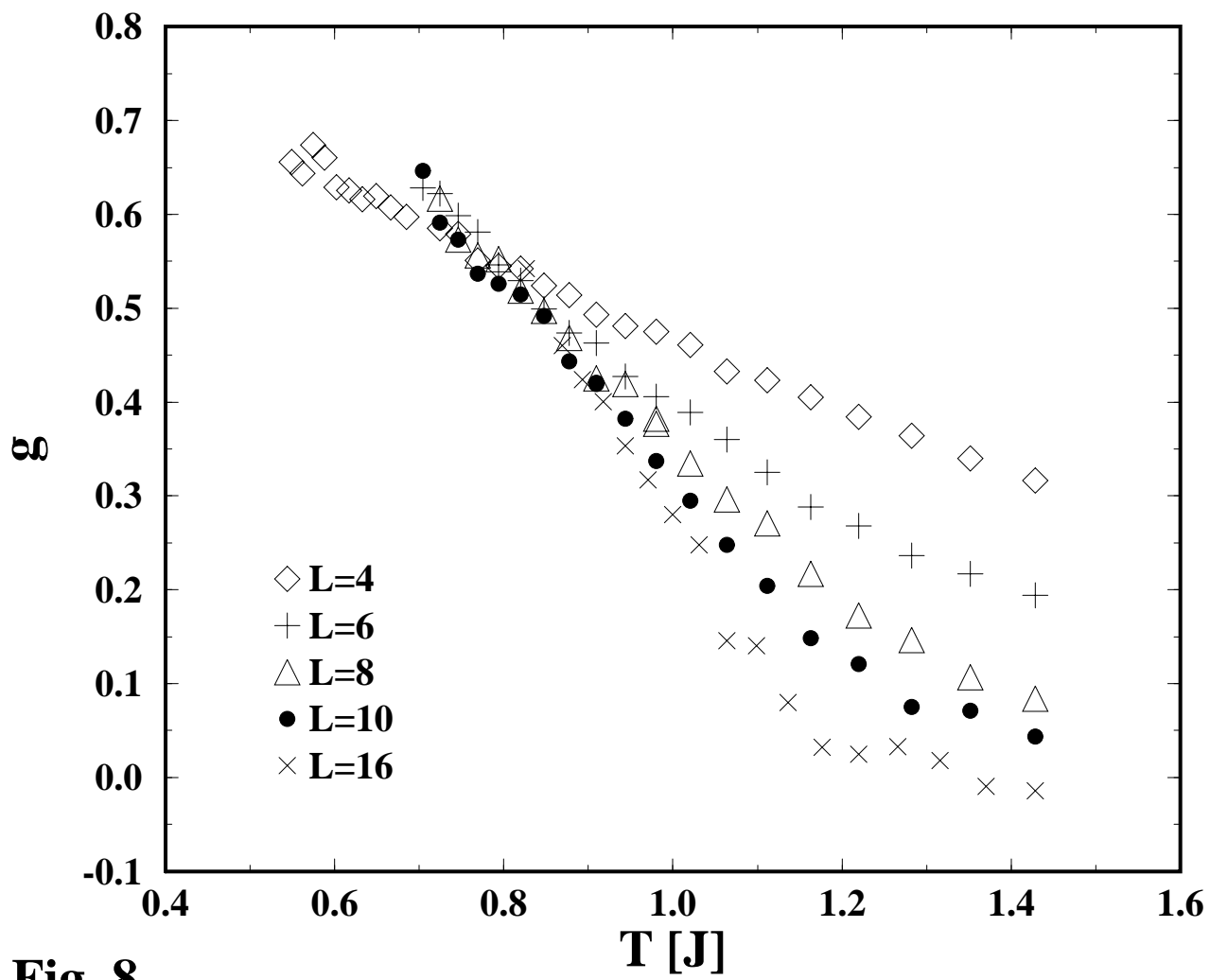


Fig. 8

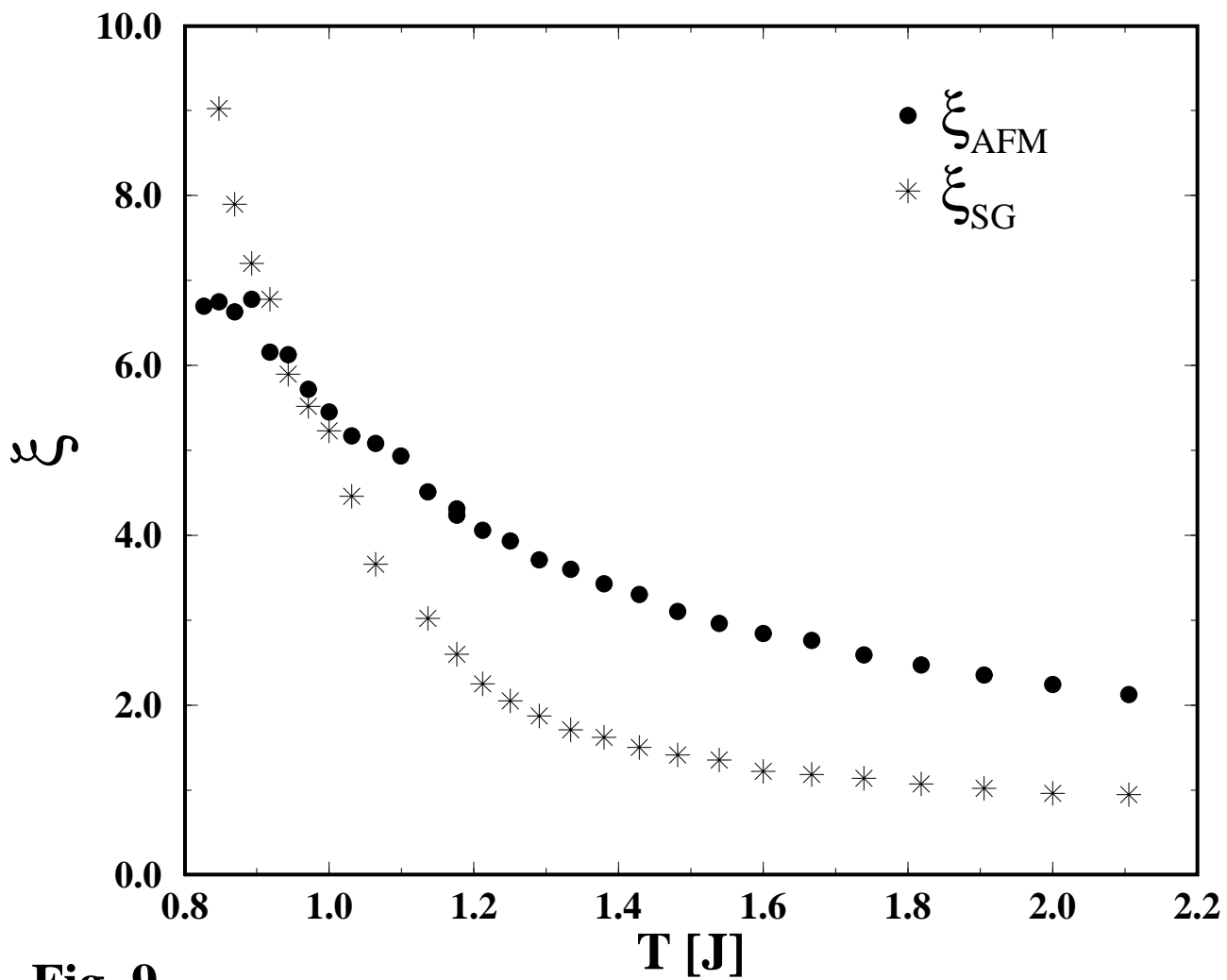


Fig. 9

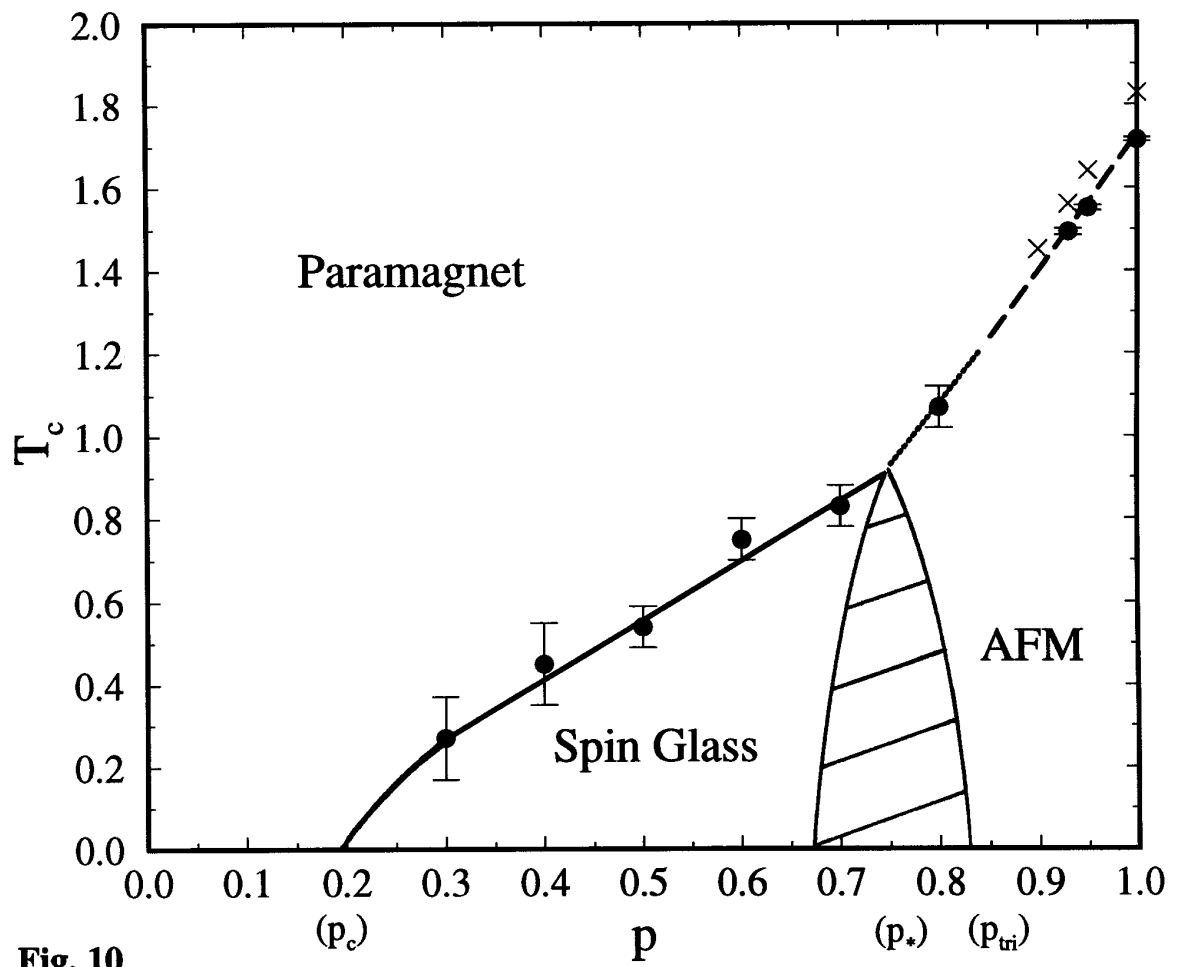


Fig. 10